An analysis of annular fin's thermal conductivity and heat production using the DTM-Pade approximation

Deepak Umarao Sarwe[1], Vishnu Sharma[2], Pradip Kumar Gaur*[2] and Stephan Antony Raj[3]

[1]Department of Mathematics, University of Mumbai, Maharastra, 40098, India

[2] Department of Mathematics, JECRC University, Jaipur, 303905, India

[3]Department of Mathematics, Rathinam Group of Institutions, Tamil nadu, 641107, India

[1] *deepaksarve@mathematica.mu.ac.in*

[2] *vishnu83.sharma@gmail.com*

*[2] *pradeep.gaur@jecrcu.edu.in*

[3] *stephanraj138@gmail.com*

Abstract

The DTM-Pade approximation is used in the current work to analyze the thermal behavior and thermal stresses of an annular fin while accounting for temperature-dependent thermal conductivity and internal heat generation. The energy problem is converted into a nonlinear ordinary differential equation (ODE) using non-dimensional parameters, and the DTM-Pade approximation is then utilized to provide an approximate analytical solution. The impacts of various settings on the temperature field are also graphically analyzed. It has been found that increasing the heat generation parameter causes the temperature distribution to improve. The growing thermo-geometric parameter values lead to an improvement in fin efficiency.

Keywords: Annular fin; DTM-Pade approximant method; Heat generation.

Nomenclature:

r_0	Outer radius	t	Thicknesses of the fin
Q	Actual heat transfer	$T_\star$	Temperature
h	Heat transfer coefficient	λ	Thermo-geometric parameter
α	Nondimensional heat generation	α	Heat generation parameter
κ_0	Thermal conductivity at ambient temperature	R	Dimensionless outer radius

θ	Dimensionless temperature	ν	Internal heat generation variation
q_0	Internal heat generation at ambient temperature	μ	Nondimensional heat generation variation
T_∞	Ambient temperature	k	Thermal conductivity of the fin
ζ	Dimensionless radius	T_b	Base temperature
$Q_{\max}$	Maximum possible heat transfer	r_i	Inner radius
η	Fin efficiency	κ	Thermal conductivity variation
σ_r, σ_ϕ	Radial and tangential stress	χ	Dimensionless coefficient of thermal expansion
$\alpha*$	linear coefficient of thermal expansion	ν	Poisson's ratio
$\varepsilon_r, \varepsilon_\phi$	Radial and tangential strain	$\bar{\sigma}_r, \bar{\sigma}_\phi$	Dimensionless radial and tangential stress
E	Young's modulus		

1 Introduction

Annular fins are typical heat transfer components that are employed in a variety of engineering applications to improve surface heat dissipation. The circular shape of these fins promotes effective heat transfer while using the least amount of material. In real-world situations, materials' thermal conductivities frequently change with temperature, and heat generation may take place within the fin structure for a variety of reasons. Optimizing the design and performance of annular fins with these complexities requires accurate analysis. Finned surfaces are widely used in electrical components, computer CPU heat sinks, heat exchangers, superheaters, electrical equipment, automobile radiators, compressor cylinders, and refrigeration because they can improve the convection heat transference between a solid surface and its surroundings. There are several ways to increase heat transfer, but one of the best is to mount a fin to the primary surface to offer more surface area. Numerous studies examine the behavior of thermal distribution through annular fins with standard profile shapes as triangular, rectangular, concave and hyperbolic, and convex parabolic fins. Recently, a number of researchers used numerical and analytical methods to examine the heat transfer properties of various fins. By taking into account the varied thermal conductivity, Darvishi et al. [1] investigated the thermal dispersion of an annular fin. Using a graphical illustration, Gaba et al. [2] addressed the heat transmission and effectiveness of annular fins with parabolic and exponential profiles. The differential evolution method was utilized by Ranjan et al. [3] to examine the radiative

phenomenon through an annular fin. By using the Durbin inverses Laplace transform approach, Bas and Keles [4] explained the thermal stress characteristics of one-dimensional annular extended surfaces. The property of temperature distribution across an annular fin was studied by Lee et al. in [5], and they also looked into the thermal stress of the fin. The heat distribution of a permeable fin submerged in a nanoliquid was examined by Sowmya et al. [6]. Baslem et al. [7] investigated the heat transfer of a straight porous fin positioned in a nanofluid while taking radiation and natural convection into account. The Homotopy Perturbation Method (HPM), Variational Iteration Method (VIM), Homotopy Analysis Method (HAM), and Adomian Decomposition Method (ADM) are some of the analytical techniques that can be used to address nonlinear differential problems. But the computations used in these methods are complicated. A technique that may effortlessly and without restrictions solve nonlinear terms is essential. This benefit is provided by the Differential Transformation Method (DTM), which may be used to expand a power series to find the analytical solution to differential equations that are both linear and nonlinear. By converting differential equations into algebraic equations, the numerical method known as DTM can solve differential equations. It offers an effective and precise approach to approximate the solutions of differential equations, particularly when closed-form solutions are not easily accessible. It is often used in conjunction with the Pade approximation. DTM with the Pade approximation can be used to get approximations of solutions for the temperature distribution T(r) in the context of the annular fin with temperature-dependent features. The Pade approximation is used to shorten the infinite series produced by DTM once the differential equation and boundary conditions are translated into algebraic equations. This approach expands the solution into Taylor's series form. DTM was initially used by Zhou [8] to examine an electrical circuit by solving both linear and nonlinear initial value issues. By taking varying thermal conductivity into account, Ghasemi et al. [9] were able to get at the analytical solution for the heat distribution through a fin using the DTM's attributes. In their study of the effects of radiation on a permeable extended surface (Moradi et al., [10], they used DTM to arrive at an analytical solution for the temperature field. Kundu and Lee [11] elaborated on heat transmission via an annular permeable extended surface, and DTM was used to solve the governing equation. For the temperature equation of the straight fin with varying thermal conductivity, Mosayebidorcheh et al. [12] used DTM. By using the DTM-Pade approximation, Christopher et al. [13] examined the hybrid nanoliquid stream across a cylindrical geometry. The creation of internal heat through a fin has been studied by several researchers. The significance of internal heat generation by an annular fin with temperature-dependent thermal conductivity was discussed by Ranjan and Mallick in [14]. The thermal behavior of a one-dimensional permeable rectangular fin with heat

generation was discussed by Hoseinzadeh et al. [15]. An analytical method was used by Ranjan et al. [16] to examine the thermal stresses and heat generation of an annular extended surface. By accounting for thermal conductivity, Kezzar et al. [17] investigated the features of heat generation over a longitudinal extended surface. Sowmya et al. [18] scrutinized the aspect of internal heat generation through a permeable fin immersed in a nanoliquid. The literature described above demonstrates that using the DTM-Pade approximant, no attempt has been made to examine the thermal distribution and thermal stresses of annular fins with internal heat generation and temperature-dependent thermal conductivity. A challenging issue in heat transfer and thermal engineering is analyzing the thermal behavior of an annular fin with temperature-dependent thermal conductivity and heat generation. Using a numerical method called the Differential Transformation Method (DTM) and Pade approximation, one can approximate the answers to such issues. Let's dissect the elements of this issue and talk about how DTM-Pade approximation might be used. Also, we refer [27–31] for more information. Therefore, the main goal of this inquiry is to use the DTM-Pade approximant, a sophisticated mathematical technique, to solve the annular fin's energy equation. Additionally, internal heat generation and thermal analysis of fins with temperature-dependent thermal conductivity are examined. The main advantage of this method is that it may be used directly on the issue without any linearization, perturbation, or discretization being necessary. Additionally, it offers more precise or exact solutions.

2 Formulation in mathematics

The following assumptions form the basis of the mathematical model:

1. This study takes into account an axisymmetric thin annular fin with uniform thickness, uniform inner and outer radii, and homogenous isotropic material, as shown in Figure 1.

2. The temperature of the surrounding liquid doesn't change while the heat is rejected.

3. At the tip of the fin, very little heat is lost.

4. Heat conduction only happens in the radial direction since there are no thermal gradients in the circumferential or axial orientations.

5. The base of the fin is maintained at a consistent temperature.

6. Convective heat transfer's coefficient is a fixed quantity.

7. By convection, the fin loses heat to its surroundings.

8. The fin functions in a steady condition.

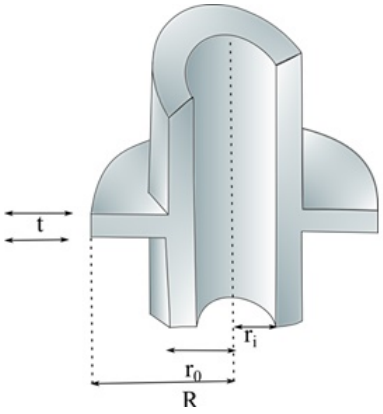

Figure 1: Schematic of an annular fin.

Under these assumptions, the energy equation derived from the law of conservation of energy for one-dimensional heat transfer is specified as [19]:

$$t\frac{d}{dr}\left[k(T_\star)r\frac{dT_\star}{dr}\right] - 2hr(T_\star - T_\infty) + q^*(T_\star)tr = 0 \tag{1}$$

The following values for the thermal conductivity and internal heat generation are assumed to change linearly with temperature:

$$\begin{aligned} k(T_\star) &= k_0\{1 + \kappa(T_\star - T_\infty)\}, \\ q^*(T_\star) &= q_0\{1 + \nu(T_\star - T_\infty)\}. \end{aligned} \tag{2}$$

Therefore, the following boundary conditions for the energy balance equation can be obtained by implementing zero conductive heat resistance at the fin wall.

$$\begin{aligned} r = r_i : T_\star = T_b, \\ r = r_0 : \tfrac{dT_\star}{dr} = 0. \end{aligned} \tag{3}$$

The following non-dimensional parameters are utilized.

$$\begin{aligned} &\theta = \frac{T_\star - T_\infty}{T_b - Ta},\ B_i = \frac{hr_i}{k_0},\ \beta = \kappa(T_b - T_\infty),\ \mu = \nu(T_b - T_\infty),\ \zeta = \frac{r - r_i}{r_i},\ R = \frac{r_0}{r_i}, \\ &\lambda^2 = \frac{2hr_i^2}{k_0 t},\ \alpha = \frac{q_0 r_i^2}{k_0(T_b - T_\infty)}. \end{aligned} \tag{4}$$

The governing equation (1) and boundary condition (3) are reduced into non-dimensional energy equation with the help of equation (2) and (4) and are given as:

$$\theta'' + \beta\theta\theta'' + \frac{\beta}{1+\zeta}\theta\theta' + \frac{1}{1+\zeta}\theta' + \beta(\theta')^2 - \lambda^2\theta + \alpha(1+\mu\theta) = 0, \tag{5}$$

$$\begin{aligned} \text{Here}, \zeta = 0 \quad &; \quad \theta = 1 \\ \text{and}, \zeta = R-1 \quad &; \quad \theta' = 0 \end{aligned} \tag{6}$$

3 Discussion on Differential Transformation Method (DTM)

The attributes of DTM were covered in this section. Using the Taylor's series expression, this method can be used to find solutions for a system of linear and nonlinear differential equations as well as adequate beginning and boundary conditions. Taylor's series has the following general form:

$$w(l) = \sum_{q=0}^{\infty} \frac{(l-l_0)^q}{q!} \left[\frac{d^q y(l)}{dx^q}\right]_{l=l_0} \tag{7}$$

The differential transformation $W(q)$ of a function $w(l)$ is expressed as follows:

$$W(q) = \frac{1}{q!}\left[\frac{d^q w(l)}{dx^q}\right]_{l=l_0} \tag{8}$$

In equation (7), $W(q)$ is the transformed function of the original function $w(l)$. Differential inverse transforms for $W(q)$ is defined as:

$$w(l) = \sum_{q=0}^{\infty} W(q)(l-l_0)^q \tag{9}$$

The fundamental properties of DTM are specified in Table. 2 (see Zhou [20], Hassan [21], Jawad and Hamody [22])

Table 2: Properties of DTM

Original function	**Transformed function**
$W(l) = g(l) \pm h(l)$	$W(q) = G(q) \pm H(q)$
$w(l) = \alpha g(l)$	$W(q) = CG(q)$, where C is the constant.

$W(l) = \frac{dh(l)}{dl}$	$W(q) = (q+1)H(q+1)$
$w(l) = \frac{d^n h(l)}{dl}$	$W(q) = (q+1)(q+1)\cdots(q+n)H(q+n)$
$w(l) = l^m$	$W(q) = \delta(q-m) = \left\{ \begin{array}{l} 1,\ q = m \\ 0,\ q \neq m \end{array} \right\}$
$w(l) = g(l)h(l)$	$W(q) = \sum_{r=0}^{q} G(r)H(q-r)$
$w(l) = f_1(l)f_2(l)\cdots$ $\cdots f_{s-1}(l)f_s(l)$	$W(q) = \sum_{q_{s-1}=0}^{q} \sum_{q_{s-2}=0}^{q_{s-1}=0} \cdots \sum_{q_2=0}^{q_3} \sum_{q_1=0}^{q_2} W_1(q_1)$ $W_2(q_2-q_1)\cdots W_{s-1}(q_{s-1}-q_{s-2})W_s(q-q_{s-1})$

4 Pade Approximant Method

The Pade approximant is a powerful approach that is frequently used in numerical analysis and scientific computing to approximate a polynomial function into rational functions of polynomials of a particular degree (see Boyd [23] and Rashidi et al. [24]). Compared to a straightforward polynomial fit, this method enables us to describe a given function with higher precision and adaptability. Assume that a power series represents the function $h(zeta)$. Using powers of a variable, in this case $zeta$, power series are a fundamental mathematics tool for expressing functions as an infinite sum of terms. When working with functions that may be roughly represented as a sum of polynomial terms, they are especially helpful.

$$h(\zeta) = \sum_{i=0}^{\infty} \gamma_i \zeta^i \tag{10}$$

Equation (4) is a vital initial step in any analysis using Pade approximants. The Pade approximant, a mathematical idea, is crucial to the discipline of numerical analysis. It is a rational fraction with a Maclaurin expansion that is intended to as closely match equation (3) as possible. In other words, Pade approximants use rational approximations, which are more computationally effective than attempting to directly compute or alter the actual equation, to provide an accurate representation of complicated functions.

$$\frac{\alpha_0 + \alpha_1\zeta + \alpha_2\zeta^2 + \cdots + \alpha_S\zeta^S}{\beta_0 + \beta_1\zeta + \beta_2\zeta^2 + \cdots + \beta_T\zeta^T} \tag{11}$$

It is believed that the numerator and denominator coefficients of equation (1) are of order $S+1$ and $T+1$, respectively. As a result, there is an independent T denominator, and independent $S+1$ numerator coefficients result in an overall $S+T+1$ unknown coefficient. This order suggests using the orders $1, \zeta, \zeta^2, \cdots, \zeta^{S+T}$ to usually fit the power series equation (3).

The representation of power series is given as:

$$\sum_{i=0}^{\infty}\gamma_i\zeta^i = \frac{\alpha_0+\alpha_1\zeta+\alpha_2\zeta^2+\cdots+\alpha_S\zeta^S}{\beta_0+\beta_1\zeta+\beta_2\zeta^2+\cdots+\beta_T\zeta^T}+o(\zeta^{S+T+1}) \quad (12)$$

$$(\beta_0+\beta_1\zeta+\beta_2\zeta^2+\cdots+\beta_S\zeta^T)(\gamma_0+\gamma_1\zeta+\gamma_2\zeta^2+\cdots) = \alpha_0+\alpha_1\zeta+\alpha_2\zeta^2+\cdots +\alpha_S\zeta^S+o(\zeta^{S+T+1}) \quad (13)$$

Comparing the coefficients of $\zeta^{S+1},\zeta^{S+2},\cdots,\zeta^{S+T}$

$$\begin{aligned}
\beta_T\gamma_{S-T+1}+\beta_{T-1}\gamma_{S-T+2}+\cdots+\beta_0\gamma_{S+1} &= 0,\\
\beta_T\gamma_{S-T+2}+\beta_{T-1}\gamma_{S-T+3}+\cdots+\beta_0\gamma_{S+2} &= 0,\\
&\cdots\cdots\\
&\cdots\cdots\\
&\cdots\cdots\\
\beta_T\gamma_T+\beta_{T-1}\gamma_{T+1}+\cdots+\beta_0\gamma_{S+T} &= 0,
\end{aligned} \quad (14)$$

To obtain the desired consistency in our mathematical framework, we define the parameter γ_i to be equal to zero. This choice plays a pivotal role in simplifying the system. When we set β_0 to be equal to 1, as stipulated in equation (5), this transforms the equation into a set of T linear equations. These linear equations represent the relationship between the various coefficients in our system, specifically, the T unknown denominator coefficients.

$$\begin{pmatrix}
\gamma_{S-T+1} & \gamma_{S-T+2} & \cdots & \gamma_{S+1}\\
\gamma_{S-T+2} & \gamma_{S-T+3} & \cdots & \gamma_{S+2}\\
\cdots & \cdots & \cdots & \cdots\\
\gamma_S & \gamma_{S+1} & \cdots & \gamma_{S+T}
\end{pmatrix}
\begin{pmatrix}
\beta_T\\ \beta_{T+1}\\ \cdots\\ \beta_S
\end{pmatrix}
=
\begin{pmatrix}
\gamma_{S+1}\\ \gamma_{S+2}\\ \cdots\\ \gamma_{S+T}
\end{pmatrix} \quad (15)$$

β_i is obtained from these equations. The numerator coefficients $\alpha_0,\alpha_1,\cdots,\alpha_S$ from equation (10) are found by equating the coefficients of $1,\zeta,\zeta^2,\cdots,\zeta^{S+T}$ such as,

$$\begin{aligned}
\alpha_0 &= \gamma_0, \\
\alpha_1 &= \gamma_1 + \beta_1\gamma_0, \\
\alpha_2 &= \gamma_2 + \beta_1\gamma_1 + \beta_2\gamma_0, \\
\cdots &\quad \cdots\cdots \\
\alpha_S &= \gamma_S + \sum_{i=1}^{min[S/T]} \beta_i\gamma_{S-i}.
\end{aligned} \tag{16}$$

The equations (15) and (16), also referred to as Pade equations, thereby yield the Pade numerator and denominator. These equations are crucial to numerical analysis, especially when it comes to approximating rational functions. They are effective tools for estimating complex functions using straightforward rational functions. In engineering and scientific computations, a particular kind of rational function approximation known as the $[S/T]$ Pade approximant is crucial. The trade-off between the degree of the numerator (S) and the degree of the denominator (T) is balanced in its development. A reference to another crucial equation that establishes the order of the Pade approximant is made in the phrase by the equation (10) . An approximation's accuracy and complexity are determined by its order. To ensure that the Pade approximant finds a compromise between accuracy and computational economy, the equation (10) offers a way for calculating its ideal order.

5 Applications of DTM-Pade method

The DTM-Pade method have several applications in a variety of scientific and technical fields. This potent mix of mathematical methods is essential for resolving difficult issues and simulating a wide range of phenomena. Applying DTM to the non-linear differential equation (2), we obtain the following expression

$$\begin{aligned}
(q+1)(q+2)\Theta[q+2] + \beta\sum_{r=0}^{q}\Theta[q-r](r+1)(r+2)\Theta[r+2] + \\
\beta\sum_{r+0}^{q}\sum_{m=0}^{r}\frac{1}{1+\delta[m-1]}\Theta[r-m](q-r+1)\Theta[q-r+1] + \\
\sum_{r=0}^{q}\frac{1}{1+\delta[m-1]}(q-r+1)\Theta[q-r+1] + \\
\beta\sum_{r=0}^{q}(q-r+1)\Theta[q-r+1](r+1)\Theta[r+1] - \lambda^2\Theta[k] + \alpha\delta[k] + \alpha\mu\Theta[k] = 0.
\end{aligned} \tag{17}$$

For the solution of difficult differential equations, the Differential Transformation Method (DTM) is applied to the boundary conditions of equations (6). With the aid of this groundbreaking mathematical method, we may better understand how the system behaves and create a precise expression that captures the complex interrelationships underlying the mathematical or physical events that are the subject of the inquiry. Applying DTM to the boundary conditions in equations (6) we obtain the following expression:

$$\Theta[0] = 1,\ \Theta[1] = a \tag{18}$$

Substituting $q = 0, 1, 2, \cdots$ so on and equation (18) in equation (17), we obtain the successive approximation as:

$$\Theta[2] = -\frac{1}{2}\frac{a^2\beta + \mu\alpha - \lambda^2 + a\beta + \alpha + a}{\beta + 1} \tag{19}$$

$$\Theta[3] = \frac{1}{12(\beta+1)^2}\begin{bmatrix} 6a^3\beta^2 + 4\mu\alpha a\beta - 4\lambda^2 a\beta + 6a^2\beta^2 - 2\mu\alpha a + 2\mu\alpha\beta \\ +6\alpha a\beta + 2\lambda^2 a - 2\lambda^2\beta + 6a^2\beta + a\beta^2 + 2\mu\alpha + 2\alpha\beta \\ -2\lambda^2 + 2a\beta + 2\alpha + a \end{bmatrix} \tag{20}$$

$$\Theta[4] = -\frac{1}{48(\beta+1)^3}\begin{bmatrix} 30a^4\beta^3 + 26\mu\alpha a^2\beta^2 - 26\lambda^2 a^2\beta^2 + 36a^3\beta^3 + 4\mu^2\alpha^2\beta \\ -8\mu\alpha\lambda^2\beta - 10\mu\alpha a^2 + 16\mu\alpha a\beta^2 + 36\alpha a^2\beta^2 + 4\lambda^4\beta \\ +10\lambda^2 a^2\beta - 16\lambda^2 a\beta^2 + 36a^3\beta^2 + 10a^2\beta^3 - 2\mu^2\alpha^2 \\ +10\mu\alpha^2\beta + 4\mu\alpha\lambda^2 + 12\mu\alpha a\beta - 10\alpha\lambda^2\beta + 20\alpha a\beta^2 - 2\lambda^2 \\ -12\lambda^2 a\beta + 20a^2\beta^2 + 3a\beta^3 - 2\mu\alpha^2 - 4\mu\alpha a + 6\alpha^2\beta \\ +2\alpha\lambda^2 + 20\alpha a\beta + 4\lambda^2 a + 10a^2\beta + 9a\beta^2 + 9a\beta + 3a \end{bmatrix} \tag{21}$$

and so on.

Where $\Theta[q]$ is the differential transform of $\theta(\zeta)$ and is the constant to be calculated by using boundary conditions.

Substituting the equations (18)-(21) in equation (9) comprising DTM, we obtain the

following equations:

$$\theta(\zeta) = 1 + a\zeta - \frac{1}{2}\frac{a^2\beta + \mu\alpha - \lambda_a^2\beta + \alpha + a}{\beta + 1}\zeta^2 + \frac{1}{12(\beta+1)^2}\begin{bmatrix} 6a^3\beta^2 + 4\mu\alpha a\beta - 4\lambda^2 a\beta \\ +6a^2\beta^2 - 2\mu\alpha a + 2\mu\alpha\beta \\ +6\alpha a\beta + 2\lambda^2 a - 2\lambda^2\beta \\ +6a^2\beta + a\beta^2 + a\beta^2 + 2\mu\alpha \\ +2\alpha\beta - 2\lambda + 2a\beta \\ +2\alpha + a \end{bmatrix}\zeta^3 - \frac{1}{48(\beta+1)^2}\begin{bmatrix} 30a^4\beta^3 + 26\mu\alpha a^2\beta^2 - 26\lambda^2 a^2\beta^2 + 36a^3\beta^3 + 4\mu^2\alpha^2\beta \\ -8\mu\alpha\lambda^2\beta - 10\mu\alpha a^2 + 16\mu\alpha a\beta^2 + 16\mu\alpha a\beta^2 + 36\alpha a^2\beta^2 \\ +4\lambda^4\beta + 10\lambda^2 a^2\beta - 16\lambda^2 a\beta^2 + 36a^3\beta^2 + 10a^2\beta^3 - 2\mu^2\alpha^2 \\ +10\mu\alpha^2\beta + 4\mu\alpha\lambda^2 + 12\mu\alpha a\beta - 10\alpha\lambda^2\beta + 20\alpha a\beta^2 - 2\lambda^4 \\ -12\lambda^2 a\beta + 20a^2\beta^2 + 3a\beta^3 - 2\mu\alpha^2 - 4\mu\alpha a + 6\alpha^2\beta + 2\alpha\lambda^2 \\ +20\alpha a\beta + 4\lambda^2 a + 10a^2\beta + 9a\beta^2 + 9a\beta + 3a \end{bmatrix}\zeta^4 + \cdots \tag{22}$$

To evaluate the value, we apply the Pade approximant to equation (22) along with boundary condition (6). We get the value of a and by substituting the constant value $a = -.9097156826,\ \alpha = 0.4,\ \mu = 0.4, \lambda = 1,\ \beta = 0.3$ in the equation (22) equation we get,

$$\theta(\zeta) = 1 - 0.9097256826\zeta + 0.5286012084\zeta^2 - 0.1192183969\zeta^3 + 0.05254461407\zeta^4 + \cdots$$

Table 3: Comparison of $\theta'(0)$ for the numerical method and DTM-Pade approximation

Parameters	**Numerical solution**	**DTM-Pade solution**
$\beta = 0.3$	-0.39096	-0.40052
$\alpha = 0.5$	-0.26968	-0.25435
$\mu = 0.8$	-0.26007	-0.26120
$\lambda = 1.5$	-1.13261	-1.12958

Table 4: Comparison of $\theta'(0)$ when $\mu = 0, \alpha = 0,\ \lambda = 1,\ \beta = 0.3$ for the numerical method and DTM-Pade approximation

Non dimensional radius ζ	**Arslanturk FDM [25]**	**Mallick et. al** HPM [26]	**Present DTM**
0	1.0	1.0	1.0
.1	.9477	.9455	.9489
.2	.9036	.9013	.9025
.3	.8668	.8659	.8608
.4	.8365	.8380	.8239

6 Fin Efficiency

The fin efficiency, a critical parameter for assessing a fin's thermal performance. Because it enables us to assess and improve the performance of heat exchangers, radiators, and other systems that depend on fins for heat transmission, the fin efficiency concept is useful in engineering and thermal design. Engineers can choose materials, fin geometry, and other design characteristics to increase heat transfer while minimizing energy use and material usage by having a thorough understanding of a fin's efficiency. In essence, it aids in the effective design of systems where heat absorption or dissipation is crucial for overall performance. Considerations for an annular fin's non-dimensional fin efficiency include its thickness, thermal conductivity, and outer and inner radii. We can use this equation to calculate the annular fin's efficiency at transferring heat from its base to the environment around it while taking into account its geometric and material characteristics. The non-dimensional form of fin efficiency is provided as follows for an annular fin:

$$\eta = \frac{Q}{Q_{max}} = \frac{4\pi h \int_{r_i}^{r_0} (T_\star - T_\infty) r dr}{2\pi h (r_0^2 - r_i^2)(T_b - T_\infty)} = \frac{2\int_0^{R-1} (1+\zeta)\theta d\zeta}{(R^2-1)} \tag{23}$$

7 Thermal stress formulation

A temperature gradient is applied to the annulus in the material under inquiry along its radial direction. The primary cause of stresses is an incompatible eigen-strain brought on by phase transformation, precipitation hardening, and temperature change brought on by the presence of a conduction-convection field. Furthermore, it is assumed that the only factor responsible for the evolution of the eigen-strain is the variation in temperature in the radial direction. Since the thickness of fin is significantly thinner than the radius of the fin, the difference in stress and displacement over the thickness is ignored. Additionally, due to the symmetric behavior of the issue, the radial and tangential stresses are independent of ϕ and cannot be influenced by it. As a result, the issue at hand is axisymmetrically

planar tension. The stress equilibrium equation in a cylindrical coordinate system derived from the classical theory of elasticity is as follows since the body force and inertia force are disregarded:

$$\frac{d\sigma_r}{dr} + \frac{\sigma_r - \sigma_\phi}{r} = 0 \tag{24}$$

Where σ_r and σ_ϕ are radial and tangential components of stress field.
The fin is subjected to thermal stresses, which causes the overall strain to evolve by two strains. While the second is a result of free thermal expansion, the first is caused by induced stresses. Using the traditional theory of elasticity, the stress-strain-temperature relationship is defined by the following expression:

$$\begin{aligned} \epsilon_r &= \frac{1}{E}[\sigma_r - v\sigma_\phi] + \alpha^* T_\star \\ \epsilon_\phi &= \frac{1}{E}[\sigma_\phi - v\sigma_r] + \alpha^* T_\star \end{aligned} \tag{25}$$

where ϵ_r and ϵ_ϕ represents the radial and tangential strain components, α^* is the coefficient of thermal expansion, v is the Poisson's ratio, and E is the modulus of elasticity of fin material. These parameters mentioned in the sentence play vital roles in characterizing the behavior of a material or a structural element.
Equation (25) can be written in the form

$$\begin{bmatrix} \sigma_r \\ \sigma_\phi \end{bmatrix} = \frac{E}{1-v^2} \begin{bmatrix} 1 & v \\ v & 1 \end{bmatrix} \begin{bmatrix} \epsilon_r \\ \epsilon_\phi \end{bmatrix} - \frac{E\alpha^* T_\star}{1-v} \begin{bmatrix} 1 \\ 1 \end{bmatrix} \tag{26}$$

Kinematics relations for the polar strain components, in a plane strain state, are

$$\epsilon_r = \frac{\partial u_r}{\partial r} \text{ and } \epsilon_\phi = \frac{u_r}{r} \tag{27}$$

Substituting Eqs. (27) and (26) into Eq. (24) and integrating twice, the following closed-form solution for the radial displacement is achieved as

$$u_r = \frac{(1+v)\alpha^*}{r} \int_a^r (T_\star - T_\infty)\eta d\eta + A_1 r + \frac{A_2}{r} \tag{28}$$

The traction-free boundary condition at outer and inner surfaces of the fin can be taken as

$$r = a, b : \sigma_r = 0 \tag{29}$$

Using Eqs. (28), (27), and (26), the constants of integration and can be appraised by applying the boundary conditions (Eq. 29)

$$A_1 = \frac{(1-v)a^*}{b^2-a^2}\int_a^b (T_\star - T_\infty)\eta d\eta + \alpha T_\infty \text{ and } A_2 = \frac{(1+v)a^* a^2}{b^2-a^2}\int_a^b (T_\star - T_\infty)\eta d\eta \quad (30)$$

Using the values of A_1 and A_2 from Eq. (30) in Eq. (28). We get,

$$\sigma_r = -\frac{\alpha^* E}{r^2}\int_a^r (T_\star - T_\infty)\eta d\eta + \frac{\alpha^* E}{b^2-a^2}\left(1-\frac{a^2}{r^2}\right)\int_a^b (T_\star - T_\infty)\eta d\eta \text{ and} \quad (31)$$

$$\sigma_\phi = 1\alpha^* E(T_\star - T_\infty)\int_a^r (T_\star - T_\infty)\eta d\eta + \frac{\alpha^* E}{b^2-a^2}\left(1+\frac{a^2}{r^2}\right)\int_a^b (T_\star - T_\infty)\eta d\eta. \quad (32)$$

Let us utilize the non-dimensional parameters:

$$\bar{\sigma}_r = \frac{\sigma_r}{E},\ \bar{\sigma}_\phi = \frac{\sigma_\phi}{E},\ \zeta_1 = \frac{r}{a},\ R = \frac{b}{a},\ \theta = \frac{T_\star - T_\infty}{T_b - T_\infty},\ \text{and } \chi = \alpha(T_b - T_\infty) \quad (33)$$

Using Eq. (33) in Eqs. (31) and (32) results as follows:

$$\begin{aligned}\bar{\sigma}_r &= -\frac{\alpha^*}{\zeta_1^2 a^2}(T_b - T_\infty)\int_1^{\zeta_1}\theta\cdot a\zeta_1\cdot a d\zeta_1 \\ &\quad + \frac{\alpha^*}{b^2-a^2}(T_b - T_\infty)\left(1-\frac{1}{\zeta_1^2}\right)\int_1^R \theta\cdot a\zeta_1\cdot a d\zeta_1 \quad (34)\\ \bar{\sigma}_\phi &= -\alpha^*(T_b - T_\infty) + \frac{\alpha^*}{\zeta_1^2 a^2}(T_b - T_\infty)\int_1^{\zeta_1}\theta\cdot a\zeta_1\cdot a d\zeta_1 + \\ &\quad \frac{\alpha^*}{b^2-a^2}(T_b - T_\infty)\left(1-\frac{1}{\zeta_1^2}\right)\int_1^R \theta\cdot a\zeta_1\cdot a d\zeta_1 \quad (35)\end{aligned}$$

Introduction of χ and R reduces Eqs. 34 and 35 to

$$\bar{\sigma}_r = \frac{\chi}{\zeta_1^2}\int_1^{\zeta_1}\theta\zeta_1 d\zeta_1 + \frac{\chi(\zeta_1^2-1)}{(R^2-1)\zeta_1^2}\int_1^R \theta\zeta_1 d\zeta_1 \quad (36)$$

$$\bar{\sigma}_\phi = -\chi\theta + \frac{\chi}{\zeta_1^2}\int_1^{\zeta_1}\theta\zeta_1 d\zeta_1 + \frac{\chi(\zeta_1^2+1)}{(R^2-1)\zeta_1^2}\int_1^R \theta\zeta_1 d\zeta_1 \quad (37)$$

The relation between ζ and ζ_1

$$\zeta = \zeta + 1 \quad (38)$$

Thus, the stress equations in terms of non-dimensional radius, ζ becomes

$$\bar{\sigma}_r = -\frac{\chi}{(\zeta+1)^2}\int_0^{\zeta}\theta(\zeta_+1)d\zeta + \frac{\chi(\zeta^2+2\zeta)}{(R^2-1)(\zeta+1)^2}\int_0^{R-1}\theta(\zeta+1)d\zeta \quad (39)$$

$$\bar{\sigma}_\phi = -\chi\theta + \frac{\chi}{(\zeta+1)^2}\int_0^{\zeta}\theta(\zeta_+1)d\zeta + \frac{\chi(\zeta^2+2\zeta+2)}{(R^2-1)(\zeta+1)^2}\int_0^{R-1}\theta(\zeta+1)d\zeta \quad (40)$$

8 Results and discussions

The impact of various non-dimensional parameters such as β, μ, α, and λ on dimensionless temperature field θ are elaborated graphically here. Additionally, the graphs are set up to talk about the effectiveness of an annular fin. Additionally, for the solutions found using both the DTM-Pade approximation method and the numerical method, graphs depicting variations in heat distribution are generated. The results of the numerical method will match the graphics produced by the DTM-Pade approximation method. The values of $\theta'(0)$ for various non-dimensional parameters are tabulated in Table 2 and the values obtained by DTM-Pade approximation method are closer to the values of numerical method. Table 3 epitomizes the numerical values of thermal field of an annular fin. The values obtained by DTM-Pade approximation method are tabulated and compared with existing work.

Figure 2 and Figure 3 show the effect of β on θ for both DTM-Pade approximation method and the numerical method. In Figure 2, the behavior of thermal distribution for different values of $\beta(= -0.4, -0.2, 0, 0.2, 0.4)$ is portrayed by plotting the graphs for both numerical and DTM-Pade approximation. From this figure, one can conclude that increase in the β value enhances the θ . The nature of θ for diverse values of $\beta(= 0.1, 0.2, 0.3, 0.4, 0.5)$ is explained via Figure 3 by using DTM-Pade approximation. It is found that θ upsurges for the rise in values. The variance in the thermal profile θ for various values of μ is exposed in Figure 4 and Figure 5. Figure 4 reveals the consequence of $\mu(= 0.3, 0.4, 0.5, 0.6)$ on θ for both numerical method and DTM-Pade approximation. This figure shows that as the μ values upsurges θ enhance rapidly. The aspect of θ for different values of $\mu(= 0.4, 0.5, 0.6, 0.7, 0.8)$ is explained via Figure 5 by using the DTM-Pade approximation. It indicates that increment of μ values improves the thermal distribution rate. Figure 6 and Figure 7 signify the influence of on temperature field θ by using both numerical and DTM-Pade approximation. The major impact of $\alpha(= 0.3, 0.4, 0.5, 0.6)$ on θ is elucidated in Figure 6. It denotes that, rise in the α values will enhance the temperature distribution. Furthermore, the impact of $\alpha(= 0.3, 0.4, 0.5, 0.6)$ on θ by implementing DTM-Pade approximation is shown in Figure 7. This figure reveals that, θ improves for enhanced α values.

The Three-dimensional (3D) and two-dimensional (2D) graphs are plotted (Figures 8 to Figure 15) for illustrating the variation of thermal profile for various increased values of non-dimensional parameters. Figure 8 and Figure 9 show the nature of θ for improved values of μ and β . These figures indicate that, θ enhances remarkably for enhanced values of μ and β. The major consequence of μ and α on θ is illustrated by utilizing 3D and 2D plots as shown in Figure 10 and Figure 11. These figures ensure that the improvement of μ and α values leads to the enhancement of θ . Figure 12 and Figure 13 demonstrate the behavior of μ for rising in α and values. These figures signify that, θ upsurges with the improvement of α and β values. The physical parameters influencing the efficiency of fin are discussed graphically as displayed in Figure 14 and Figure 15. The efficiency of fin is more for higher values of λ and β . Figures 16,17 and Figure 18,19 portray the aspects of thermal stresses caused due to heat transfer through the annular fin. Figure 16 and Figure 17 signifies the effect of non-dimensional parameters χ and β on radial stress distribution. Here, the radial stress magnitude upsurges with the decline of β. This happens due to the fact that, decrease in β values increases the thermal resistance. As a result, the fin material's local free expansion is hindered. Furthermore, the radial stress fields are unaffected by the heat generation factors α and
mu. Figures 10(a) and 10(b) show the impact of the non-dimensional parameters α and μ on the distribution of tangential stress. Tangential stress is significantly impacted by all non-dimensional parameters, including the heat generation parameters α and μ. For increased values of α and μ, the effect of heat generation on the tangential stresses remarkably increases.

9 Final remarks

In conclusion, it is a challenging task to analyze the thermal behavior of an annular fin with temperature-dependent thermal conductivity and heat generation. To achieve precise solutions, it is necessary to combine mathematical modeling, numerical techniques like DTM, and approximations like the Pade approximation. In many technical applications where effective heat transport and temperature control are critical, this analysis is crucial. The challenge of conducting a complex yet crucial thermal analysis of annular fins with temperature-dependent thermal conductivity and heat generation is one that engineers and designers must do. These fins can be optimized for better performance and efficiency with the use of accurate temperature distribution predictions within them. Engineers and scientists are able to effectively solve the governing equations and get insightful knowledge regarding the behavior of annular fins under real-world circumstances by using mathematical methods like the Differential Transformation Method (DTM) and Pade

approximation. Making informed judgments on the design and application of such heat transfer devices across a range of applications is made easier with the help of this analysis, which improves energy efficiency and system performance.

Utilizing the DTM-Pade approximant method, the current study investigates the heat transference analysis as well as the thermal stresses aspect of an annular fin with temperature-dependent thermal conductivity. Additionally, the current approach yields findings for the thermal field. According to the results of this study, the DTM-Pade approximant-based method offers fairly precise results and is easier to manage the nonlinear problem. From the current investigation, it is possible to draw the following conclusions:

- The thermal distribution is enhanced by the increasing values of β.
- The thermal distribution increases as μ values rise. Additionally, α is increased by the thermal distribution function.
- The effectiveness of the fin is increased by the rising values of non-dimensional parameters λ.
- The magnitude of the radial stress increases as β declines.
- For increased values of α and μ, the effect of heat generation on the tangential stresses remarkably increases.

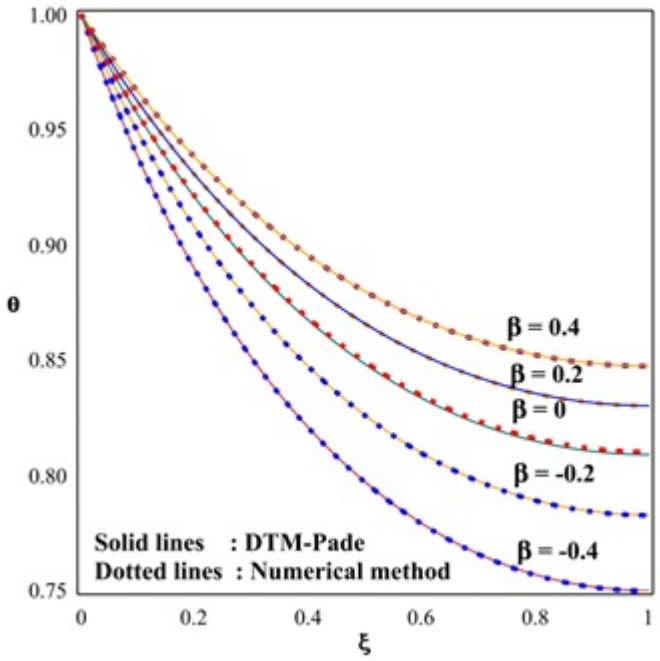

Figure 2: Influence of β on θ.

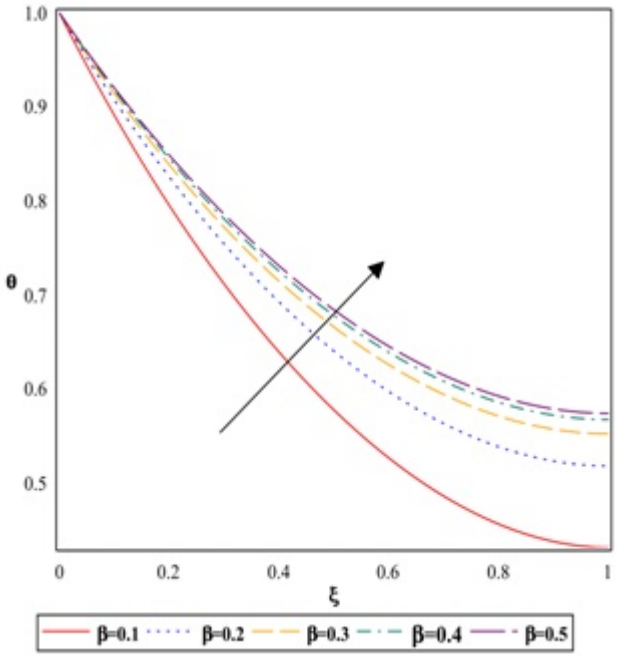

Figure 3: Influence of β on θ by using DTM-Pade Approximation.

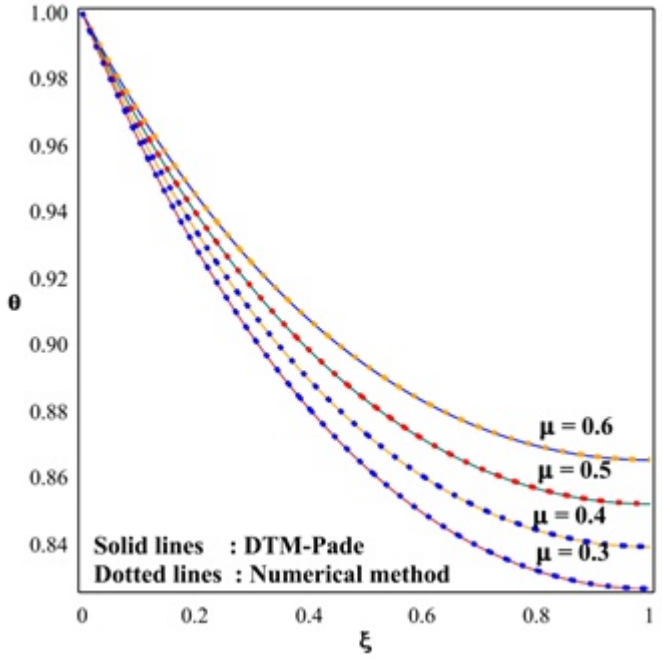

Figure 4: Influence of μ on θ.

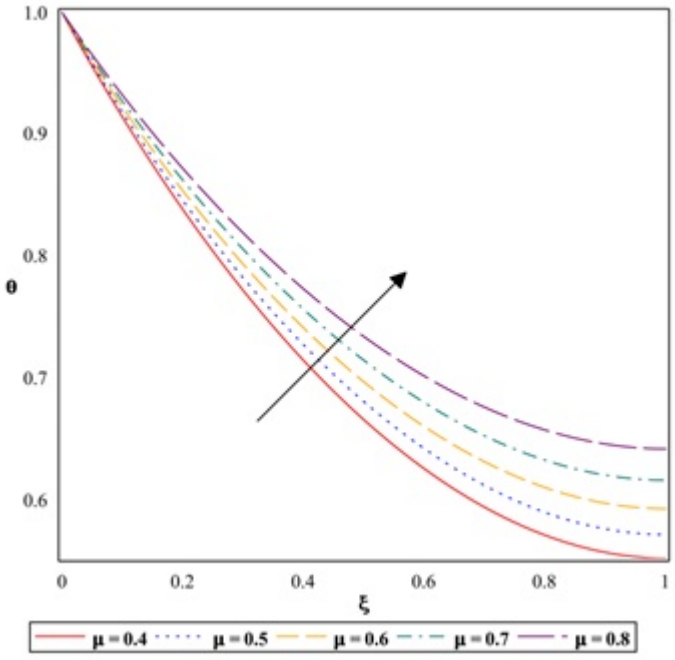

Figure 5: Influence of μ on θ by using DTM-Pade Approximation.

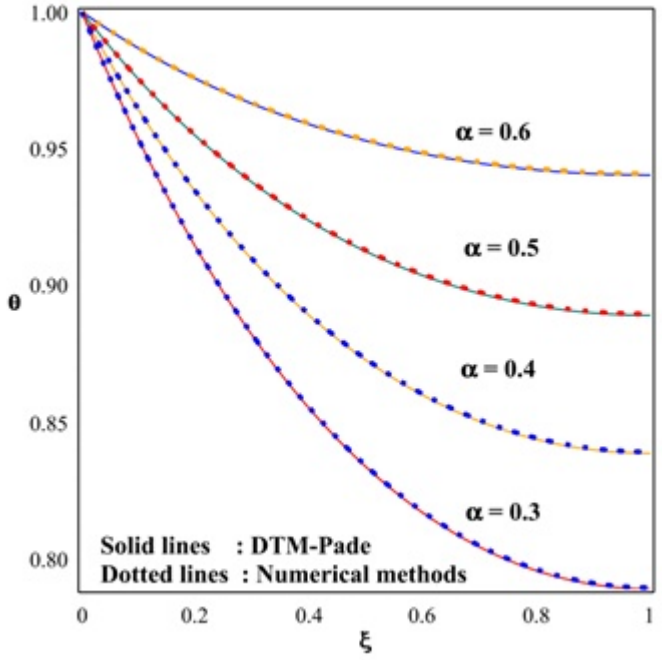

Figure 6: Influence of α on θ.

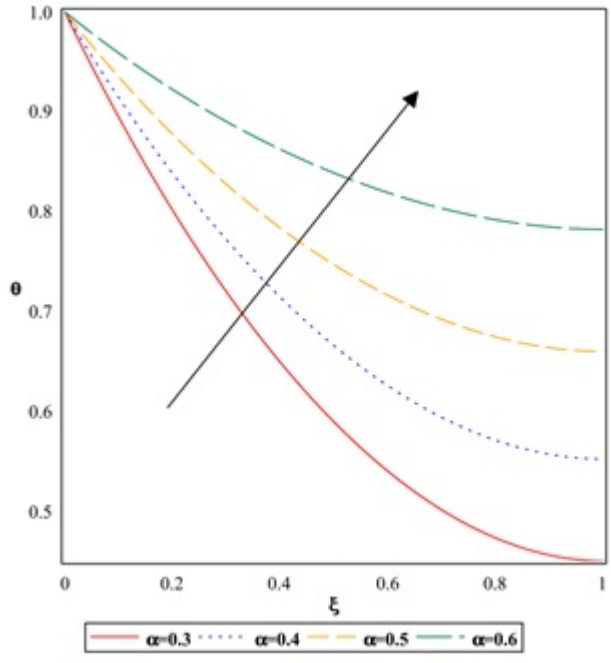

Figure 7: Influence of α on θ by using DTM-Pade Approximation.

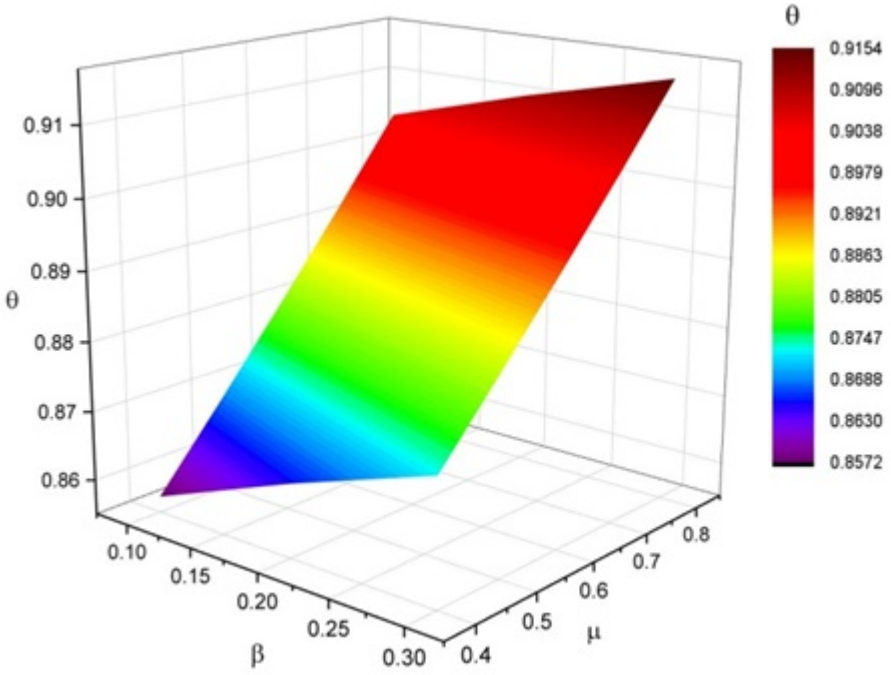

Figure 8: Deviance of θ for diverse values of μ against β.

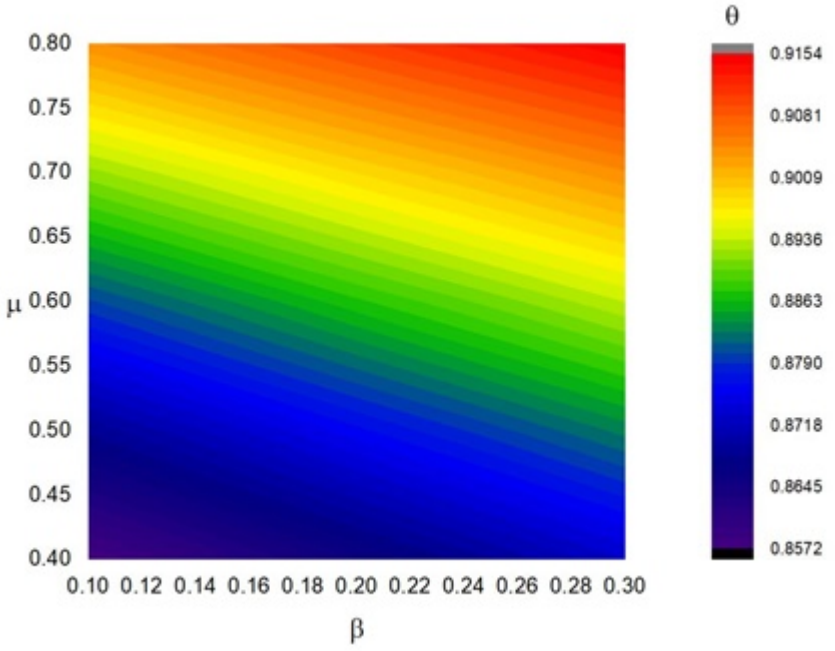

Figure 9: Deviance of θ for diverse values of μ against β.

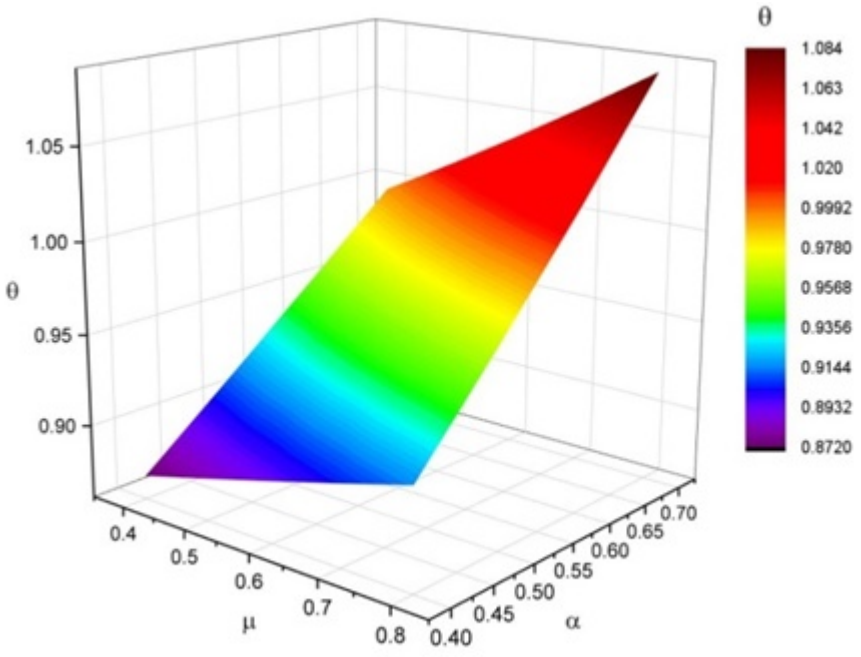

Figure 10: Deviance of θ for diverse values of μ against α.

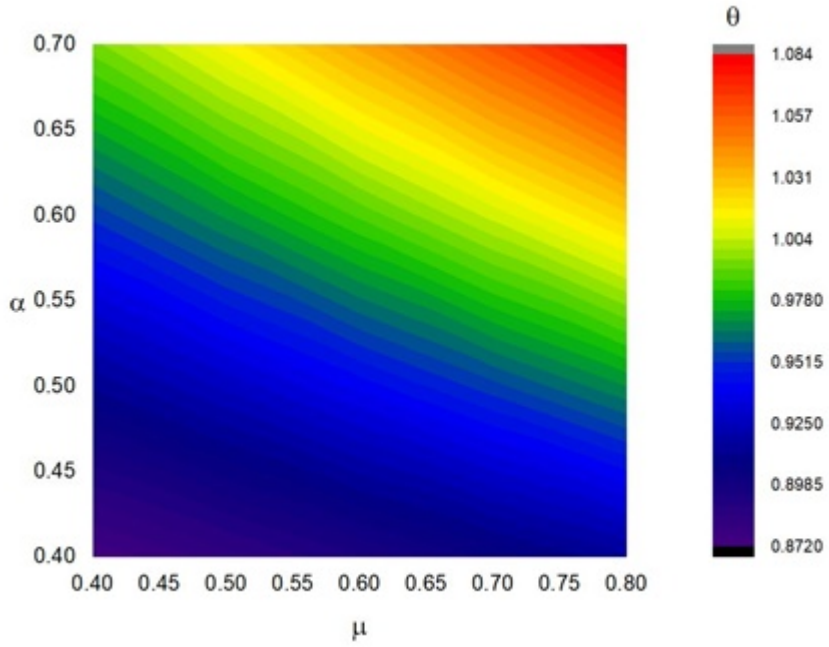

Figure 11: Deviance of θ for diverse values of μ against α.

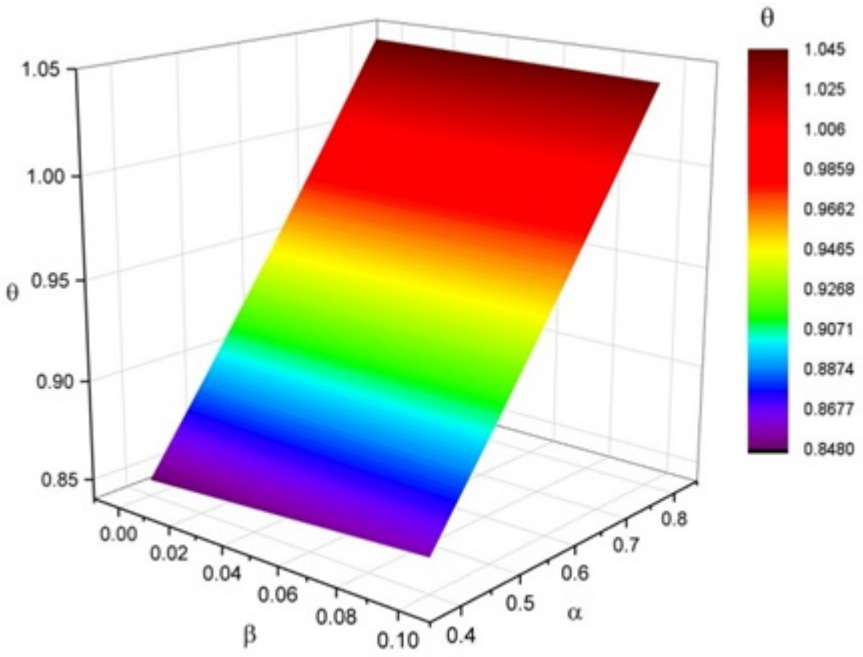

Figure 12: Deviance of θ for diverse values of α against β.

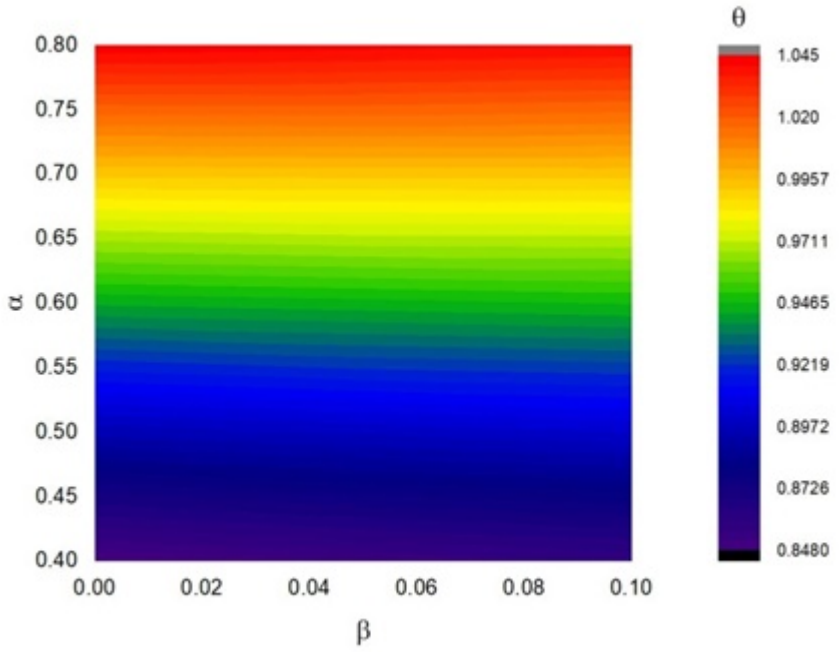

Figure 13: Deviance of θ for diverse values of α against β.

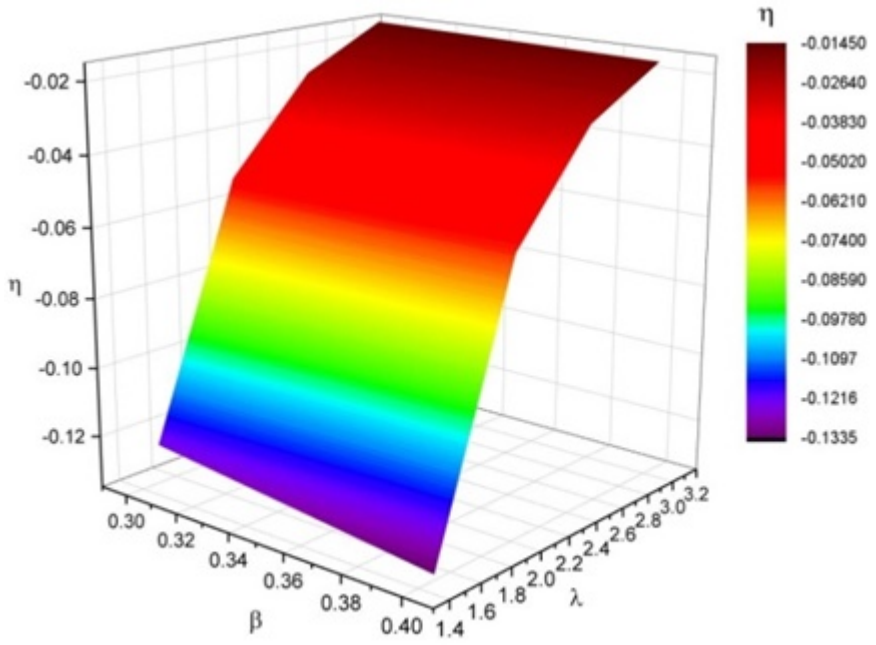

Figure 14: Efficiency of fin ν for diverse values of λ against β.

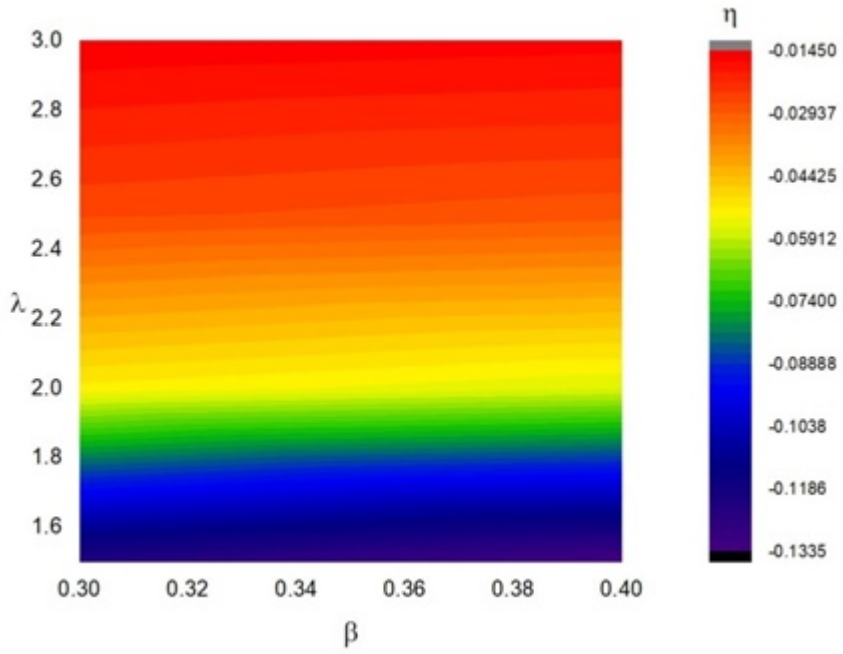

Figure 15: Efficiency of fin ν for diverse values of λ against β.

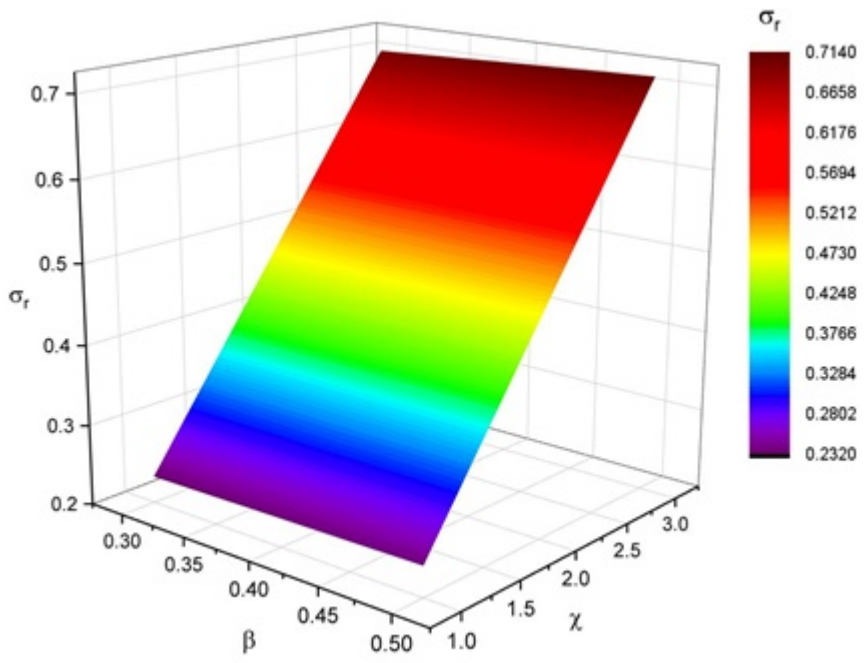

Figure 16: Impact of non-dimensional parameters χ and β on radial stress distribution.

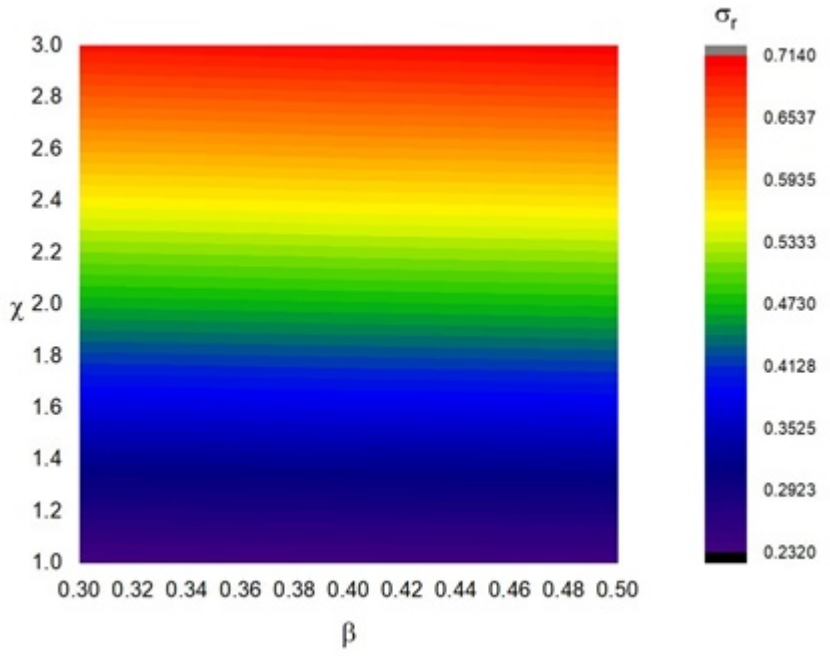

Figure 17: Impact of non-dimensional parameters χ and β on radial stress distribution.

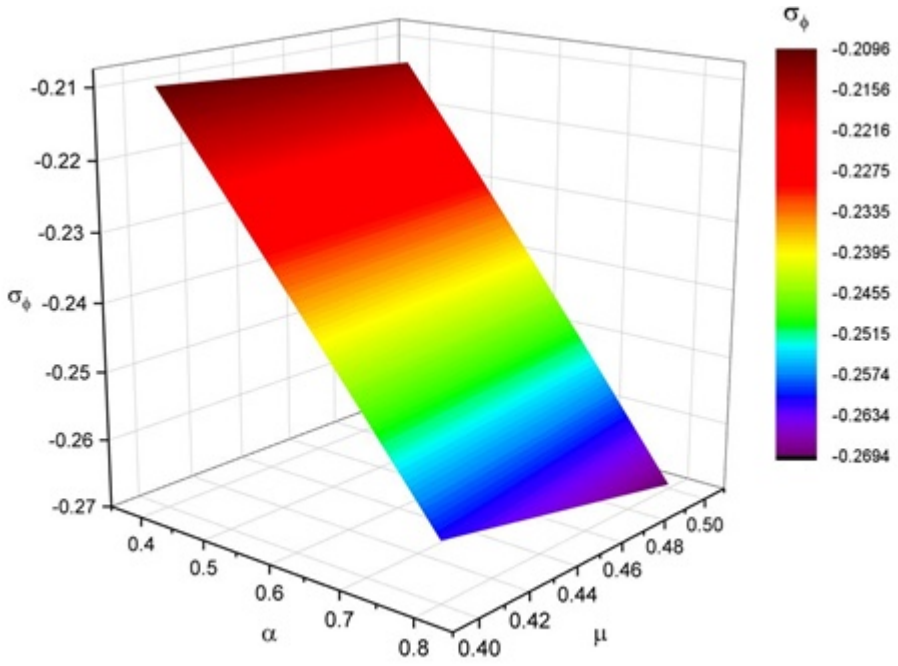

Figure 18: Impact of non-dimensional parameters α and μ on tangential stress distribution.

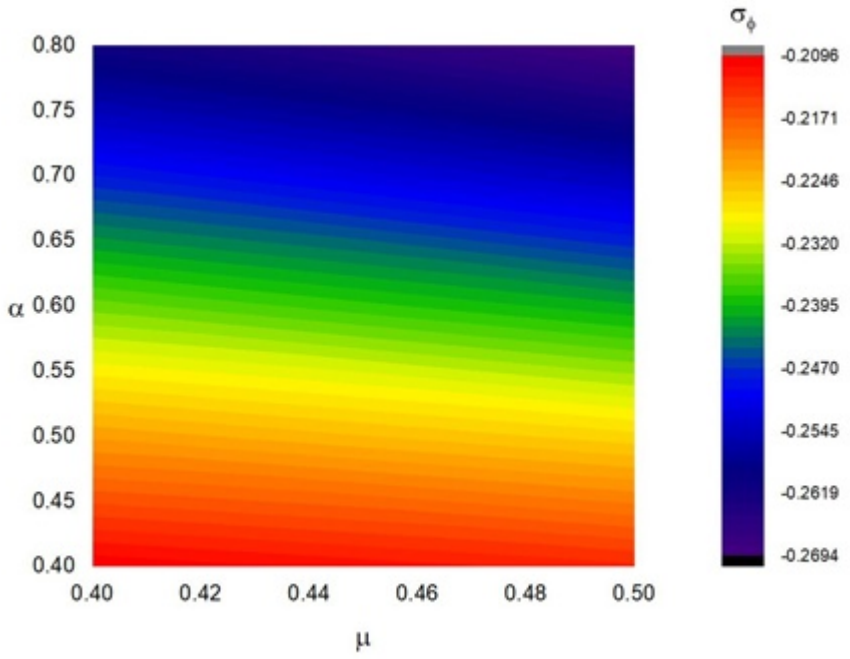

Figure 19: Impact of non-dimensional parameters α and μ on tangential stress distribution.

References

[1] M. T. Darvishi, F. Khani, and A. Aziz, "Numerical investigation for a hyperbolic annular fin with temperature-dependent thermal conductivity," Propuls. Power Res., vol. 5, no. 1, pp. 55–62, Mar. 2016, doi: 10.1016/j.jppr.2016.01.005.

[2] V. Gaba, A. Tiwari, and S. Bhowmick, "A report on performance of annular fins having varying thickness," J. Eng. Appl. Sci., vol. 11, pp. 5120–5125, Apr. 2016.

[3] R. Ranjan, A. Mallick, and D. K. Prasad, "Closed form solution for a conductive–convective–radiative annular fin with multiple nonlinearities and its inverse analysis," Heat Mass Transf., vol. 53, no. 3, pp. 1037–1049, Mar. 2017, doi: 10.1007/s00231-016-1872-8.

[4] H. Bas and İ. Keles, "Analysis of Transient Thermal Stresses in Annular Fin," presented at the The 2nd World Congress on Momentum, Heat and Mass Transfer, Apr. 2017, doi: 10.11159/ichtd17.103.

[5] S.-Y. Lee, L.-K. Chou, and C. K. Chen, "Nonlinear temperature and thermal stress analysis of annular fins with time dependent boundary condition," Eng. Comput., vol. 35, no. 3, pp. 1444–1459, Jan. 2018, doi: 10.1108/EC-07-2017-0289.

[6] G. Sowmya, B. J. Gireesha, B. C. Prasannakumara, "Scrutinization of different shaped nanoparticle of molybdenum disulfide suspended nanofluid flow over a radial porous fin," Int. J. Numer. Methods Heat Fluid Flow, vol. 30, no. 7, pp. 3685–3699, Jan. 2019, doi: 10.1108/HFF-08-2019-0622.

[7] A. Baslem, G. Sowmya, B. J. Gireesha, B. C. Prasannakumara, M. Rahimi-Gorji, and N. M. Hoang, "Analysis of thermal behavior of a porous fin fully wetted with nanofluids: convection and radiation," J. Mol. Liq., vol. 307, p. 112920, Jun. 2020, doi: 10.1016/j.molliq.2020.112920.

[8] J. K. Zhou, Differential transformation and its applications for electrical circuits. Huazhong University Press, Wuhan, China, 1986.

[9] S. E. Ghasemi, M. Hatami, and D. D. Ganji, "Thermal analysis of convective fin with temperature-dependent thermal conductivity and heat generation," Case Stud. Therm. Eng., vol. 4, pp. 1–8, Nov. 2014, doi: 10.1016/j.csite.2014.05.002.

[10] A. Moradi, T. Hayat, and A. Alsaedi, "Convection-radiation thermal analysis of triangular porous fins with temperature-dependent thermal conductivity by DTM," Energy Convers. Manag., vol. 77, pp. 70–77, Jan. 2014, doi: 10.1016/j.enconman.2013.09.016.

[11] B. Kundu and K.-S. Lee, "A proper analytical analysis of annular step porous fins for determining maximum heat transfer," Energy Convers. Manag., vol. 110, pp. 469–480, Feb. 2016, doi: 10.1016/j.enconman.2015.09.037.

[12] S. Mosayebidorcheh, M. Farzinpoor, and D. D. Ganji, "Transient thermal analysis of longitudinal fins with internal heat generation considering temperature-dependent properties and different fin profiles," Energy Convers. Manag., vol. 86, pp. 365–370, Oct. 2014, doi: 10.1016/j.enconman.2014.05.033.

[13] A. J. Christopher, N. Magesh, R. J. P. Gowda, R. N. Kumar, and R. S. V. Kumar, "Hybrid nanofluid flow over a stretched cylinder with the impact of homogeneous–heterogeneous reactions and Cattaneo–Christov heat flux: Series solution and numerical simulation," Heat Transf., vol. n/a, no. n/a, doi: https://doi.org/10.1002/htj.22052.

[14] R. Ranjan and A. Mallick, "An Efficient Unified Approach for Performance Analysis of Functionally Graded Annular Fin with Multiple Variable Parameters," Therm. Eng., vol. 65, no. 9, pp. 614–626, Sep. 2018, doi: 10.1134/S0040601518090082.

[15] S. Hoseinzadeh, A. Moafi, A. Shirkhani, and A. J. Chamkha, "Numerical Validation Heat Transfer of Rectangular Cross-Section Porous Fins," J. Thermophys. Heat Transf., vol. 33, no. 3, pp. 698–704, 2019, doi: 10.2514/1.T5583.

[16] R. Ranjan, A. Mallick, and P. Jana, "Thermoelastic study of a functionally graded annular fin with variable thermal parameters using semiexact solution," J. Therm. Stress., vol. 42, no. 10, pp. 1272–1297, Oct. 2019, doi: 10.1080/01495739.2019.1646617.

[17] M. Kezzar, I. Tabet, and M. R. Eid, "A new analytical solution of longitudinal fin with variable heat generation and thermal conductivity using DRA," Eur. Phys. J. Plus, vol. 135, no. 1, p. 120, Jan. 2020, doi: 10.1140/epjp/s13360-020-00206-0.

[18] G. Sowmya, B. J. Gireesha, S. Sindhu, and B. C. Prasannakumara, "Investigation of Ti6Al4V and AA7075 alloy embedded nanofluid flow over longitudinal porous fin in the presence of internal heat generation and convective condition," Commun. Theor. Phys., vol. 72, no. 2, p. 025004, Feb. 2020, doi: 10.1088/1572-9494/ab6904.

[19] A. Mallick, R. Ranjan, D. K. Prasad, and R. Das, "Inverse Prediction and Application of Homotopy Perturbation Method for Efficient Design of an Annular Fin with Variable Thermal Conductivity and Heat Generation," Math. Model. Anal., vol. 21, no. 5, Art. no. 5, Sep. 2016, doi: 10.3846/13926292.2016.1225606.

[20] J. K. Zhou, Differential transformation and its applications for electrical circuits. Huazhong University Press, Wuhan, China, 1986.

[21] I. H. Abdel-Halim Hassan, "Different applications for the differential transformation in the differential equations," Appl. Math. Comput., vol. 129, no. 2, pp. 183–201, Jul. 2002, doi: 10.1016/S0096-3003(01)00037-6.

[22] A. Jawad and A. Hamody, "Differential Transformation Method for Solving Nonlinear Heat Transfer Equations," Feb. 2013. doi: 10.13140/2.1.2858.4965.

[23] J. P. Boyd, "Padé approximant algorithm for solving nonlinear ordinary differential equation boundary value problems on an unbounded domain," Comput. Phys., vol. 11, no. 3, pp. 299–303, May 1997, doi: 10.1063/1.168606.

[24] M. M. Rashidi, N. Freidoonimehr, E. Momoniat, and B. Rostami, "Study of Nonlinear MHD Tribological Squeeze Film at Generalized Magnetic Reynolds Numbers Using DTM," PLOS ONE, vol. 10, no. 8, p. e0135004, Aug. 2015, doi: 10.1371/journal.pone.0135004

[25] C. Arslanturk, "Correlation equations for optimum design of annular fins with temperature dependent thermal conductivity," Heat Mass Transf., vol. 45, no. 4, pp. 519–525, Feb. 2009, doi: 10.1007/s00231-008-0446-9.

[26] A. Mallick, S. Ghosal, P. K. Sarkar, and R. Ranjan, "Homotopy Perturbation Method for Thermal Stresses in an Annular Fin with Variable Thermal Conductivity," J. Therm. Stress., vol. 38, no. 1, pp. 110–132, Jan. 2015, doi: 10.1080/01495739.2014.981120

[27] Jangid Sanju, Mehta Ruchika, Singh Jagdev, Baleanu Dumitru and Alshomrani Ali Saleh, "Heat and mass transport of hydromagnetic williamson nanofluid passing through a permeable media across an extended sheet of varying thickness", Thermal Science, vol. 27, pp. 129-140, 2023, doiserbia.nb.rs/Article.aspx?ID=0354-983623129J.

[28] Jain Ruchi, Mehta Ruchika, Mehta Tripti, Singh Jagdev and Baleanu Dumitru, "MHD flow and heat and mass transportinvestigation over a decelerating disk with ohmic heating and diffusive effect", Thermal Science, vol. 27 (1), pp. 141-149, 2023, doiserbia.nb.rs/Article.aspx?ID=0354-983623141J.

[29] Kumar Ravindra, Singh Jagdev, Mehta Ruchika, Kumar Devendra and Baleanu Dumitru, "Analysis of the impact of thermal radiation and velocity slip on the melting

of magnetic hydrodynamic micropolar fluid-flow over an exponentially stretching sheet", Thermal Science, vol. 27 (1), pp. 311-322, 2023, doi:10.2298/TSCI23S1311K.

[30] Ruchika Mehta, Ravindra Kumar, Himanshu Rathore and Jagdev Singh, "Joule heating effect on radiating MHD mixed convection stagnation point flow along vertical stretching sheet embedded in a permeable medium and heat generation/absorption", Heat Transfer (Wiley), vol. 51 (8), pp. 7369-7386, 2022, doi: 10.1002/htj.22648.

[31] Jagdev Singh, George A. Anastassiou, Dumitru Baleanu, Carlo Cattani, and Devendra Kumar, "Analysis of Soret and Dufour Effect on MHD Fluid Flow Over a Slanted Stretching Sheet with Chemical Reaction, Heat Source and Radiation", Advances in Mathematical Modelling, Applied Analysis and Computation. Lecture Notes in Networks and Systems, Springer, Singapore, vol. 415, Oct. 2022, doi.org/10.1007/978-981-19-0179-9.